Reaction of HO_2 with ClO: Flow Tube Studies of Kinetics and Product Formation between 215 and 298 K

G. P. Knight,† T. Beiderhase, F. Helleis, G. K. Moortgat, and J. N. Crowley*

Division of Atmospheric Chemistry, Max-Planck-Institut für Chemie, Postfach 3060, 55020 Mainz, Germany

Received: July 20, 1999; In Final Form: December 3, 1999

Rate coefficients for the reaction between HO_2 and ClO radicals were obtained using the discharge-flow/mass-spectrometry technique at total pressures of 1.1−1.7 Torr of He, and between 298 and 215 K. The room-temperature rate constant, determined using seven different combinations of HO_2 and ClO precursors, was found to be $(7.1 \pm 1.8) \times 10^{-12}$ ($\pm 2\sigma$) $cm^3\ s^{-1}$. The temperature-dependent overall reaction rate coefficient is described by $k_{(3)}$ (298−215 K) = $(7.1 \pm 0.4) \times 10^{-12} \exp(-16 \pm 17/T)$ $cm^3\ s^{-1}$. The previous observation of a strong negative temperature dependence in the title reaction below 298 K was not observed, resulting in a significantly lower rate coefficient at stratospheric temperatures. HOCl was the only product of the reaction, and an upper limit of 1% for the branching ratio for the formation of O_3 and HCl was obtained at the low pressures of these experiments.

Introduction

The emission of anthropogenic chlorofluorocarbons has resulted in an increase of chlorine in the stratosphere from a natural level of 0.6 ppb to a contemporary level of almost 4 ppb.[1] The enhanced chlorine burden in the stratosphere is strongly correlated to the negative trend in ozone concentrations in the midlatitudes[2] and, more spectacularly, in the polar regions.[3] In both cases ClO radicals are involved in the O_3 depletion mechanisms.

Reactions 1, 2, 3a, and 4 represent a known catalytic O_3 destroying cycle.[4,5] This cycle accounts for ca. 30% of the halogen-controlled loss of O_3, which in turn is ca. 30% of the

$$OH + O_3 \rightarrow HO_2 + O_2 \quad (1)$$

$$Cl + O_3 \rightarrow ClO + O_2 \quad (2)$$

$$HO_2 + ClO \rightarrow HOCl + O_2 \quad (3a)$$

$$HOCl + h\nu \rightarrow OH + Cl \quad (4)$$

$$\text{net:} \quad 2O_3 \rightarrow 3O_2$$

total loss at midlatitudes in the lower stratosphere.[6] The ozone-destroying cycle involving the HO_2 + ClO reaction outlined above is particularly important in regions with elevated ClO concentrations, such as the springtime polar stratosphere.[5,7] The air in this region is denitrified due to the conversion of NO_x to HNO_3 and the removal of HNO_3 from the gas phase through formation of polar stratospheric clouds (PSC). The low levels of NO_2 in conjunction with high ClO concentrations, augmented by chlorine activation, mean that ClO becomes the major reaction partner for HO_2.

Both HO_2 and ClO take part in several other well-documented ozone-destroying cycles. The degree to which the various cycles are coupled determines the partitioning between the reactive odd chlorine species (Cl, ClO) and the reservoirs (HOCl, $ClONO_2$, HCl), and thus the rate of the halogen-initiated ozone depletion.[8] To assess the net effect on ozone chemistry, the rate constants and product branching ratios of reaction 3 need to be known, as well as their temperature and pressure dependencies. The formation of HCl and O_3 in reaction 3b can influence the ratio of HCl to ClO, and bring modeled and measured HCl concentrations closer in agreement.[9]

$$HO_2 + ClO \rightarrow HCl + O_3 \quad (3b)$$

The overall rate constant for reaction 3 has been measured in several studies.[10−15] No pressure dependence has been observed for reaction 3 at 298 K. The temperature dependence of the rate constant for reaction 3 has been measured by Stimpfle et al.[11] According to that study, $k_{(3)}$ exhibits a strong negative temperature dependence below 298 K, indicating that reaction 3 could proceed via formation of an addition complex at low temperatures.

Several studies have shown that channel 3a is the dominant reaction pathway.[13−15] The room-temperature studies place upper limits for channel 3b of between 0.3% and 2%. At colder temperatures there is evidence for increased branching to this channel. Leu et al.[15] place an upper limit of 3% at 248 K. Also, at 210 K, Finkbeiner et al.[16] measured a branching ratio of 5% ± 2%. There has been some speculation that the stabilization of HOOOCl isomers, formed as intermediates in this reaction, is also possible.[17,18]

In this paper we present new measurements of the overall rate constant and the branching ratio for the HO_2 + ClO reaction in the temperature range from 298 to 215 K. In particular, our efforts focused upon determination of the temperature dependence for this reaction in light of the pronounced negative temperature dependence observed at $T < 298$ K by Stimpfle et al.[11]

Experimental Procedures

A schematic diagram of the discharge-flow/mass-spectrometer system used in these experiments is shown in Figure 1. The

* To whom correspondence should be addressed. E-mail: crowley@mpch-mainz.mpg.de. Fax: 49-6131-305436.

† Present address: NOAA, R/E/A12, 325 Broadway, Boulder, CO 80303.

10.1021/jp9924631 CCC: $19.00
Published on Web 02/05/2000

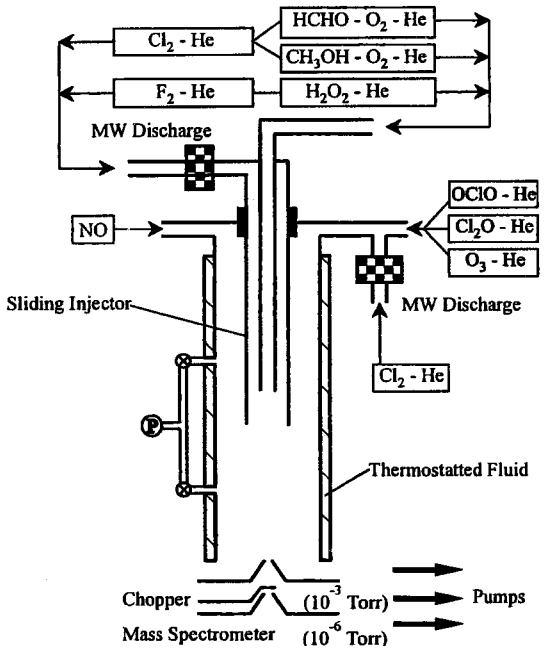

Figure 1. Schematic representation of the discharge-flow/mass-spectrometer setup showing inlet ports for the HO_2 and ClO radical precursors and NO.

main reactor is an 80 cm long by 3 cm i.d. Pyrex flow tube, the temperature of which could be controlled by passing a thermostated fluid through an outer jacket. The inner wall of the reactor was coated with halocarbon wax. This experimental setup has been discussed previously,[19] so only the salient points are given here.

The bulk flow, consisting predominantly of He, was established using calibrated flow controllers. Linear flow velocities of between 15 and 22 m s^{-1} within the reactor were then obtained by throttling a mechanical pump. Flow tube temperatures were measured using a Teflon-coated J-type thermocouple placed at the tip of the injector.

Radical and stable species, continuously sampled at the downstream end of the flow tube via a differentially pumped molecular beam interface, were detected by a mass spectrometer. Ions were generated by electron bombardment (15−30 eV, 0.05−1 mA), selected by a quadrupole mass filter (Riber/Balzers), and detected by a channeltron electron multiplier. The spectrometer was run in selective ion monitoring mode with mass-dependent variation of the ion current and signal integration times. The detection limit (S/N = 1) for HO_2 was $\sim 1 \times 10^{10}$ cm^{-3} for an integration time of 20 s.

Two microwave discharges (2450 MHz) were used for radical generation. The injector discharge (see Figure 1) was used to dissociate either F_2 or Cl_2 depending on the source chemistry employed to generate HO_2. Ceramic (Al_2O_3) inserts were used to reduce F atom reactions at the glass surface where the microwave cavity was attached to glass tubing. Low microwave power (18 W) was employed to reduce dissociation of impurities in the F_2/He or Cl_2/He mixtures. For the Cl_2 discharge a glass tube was used, which had been cleaned with 10% HF, washed with H_2O, and rinsed in H_3PO_4. The side arm discharge, used to dissociate Cl_2, was also conditioned with acid washes and run at 18 W.

Generation and Detection of HO_2 and ClO. HO_2 radicals were generated using one of three different precursor combinations in a moveable double injector concentric to the main flow tube. The sources used the reactions between CH_2OH or HCO radicals and O_2 or the reaction between H_2O_2 and F atoms.

$$CH_2OH + O_2 \rightarrow HO_2 + HCHO \quad (5a)$$

$$HCO + O_2 \rightarrow HO_2 + CO \quad (6)$$

$$F + H_2O_2 \rightarrow HO_2 + HF \quad (7)$$

CH_2OH or HCO radicals were generated by the reaction of Cl atoms with either CH_3OH or HCHO, respectively.

$$CH_3OH + Cl \rightarrow CH_2OH + HCl \quad (8)$$

$$HCHO + Cl \rightarrow HCO + HCl \quad (9)$$

The precursors, flowing as CH_3OH/O_2/He or $HCHO/O_2$/He mixtures through the innermost injector tube, were mixed in the final 16 cm of the injector with a flow of Cl atoms produced upstream by a microwave discharge of highly diluted Cl_2 in He. The H_2O_2 precursor, highly diluted with He, flowed through the innermost injector tube and then mixed in the final 16 cm with a flow of F atoms produced upstream by a microwave discharge of highly diluted F_2 in He. The inner surfaces of the injector were coated with halocarbon wax to reduce losses of atoms and radicals.

The HO_2 radical was detected as its parent ion (HO_2^+) at $m/e = 33$. For all three sources of HO_2 some correction to the raw $m/e = 33$ ion signal was necessary before a net signal attributable to HO_2 could be obtained. When using the CH_3OH/O_2 precursor pair, an interfering signal on $m/e = 33$ from the $^{13}CH_3OH$ and ^{17}OO isotopomers had to be subtracted. At 294 K the signal due to the $^{13}CH_3OH$ and ^{17}OO isotopomers was ~55% of the total $m/e = 33$ ion signal. The correction for the $HCHO/O_2$ precursor pair (from ^{17}OO) was ~30%. When using CH_3OH and HCHO as HO_2 sources, an electron energy of 20−30 eV was used, which is a compromise between strong background signals and spectrometer stability. The necessary corrections to $m/e = 33$ due to the CH_3OH/O_2 and $HCHO/O_2$ precursors could be easily measured by disabling the discharge.

The very strong fragmentation of the H_2O_2 precursor onto $m/e = 33$ at 20−30 eV electron energy made necessary a reduction to 15 eV. This resulted in a small sacrifice of spectrometer stability and sensitivity for a much reduced background signal. Typically the ion signal for H_2O_2 fragmentation onto $m/e = 33$ was around 70% of the total $m/e = 33$ ion signal at 15 eV. The fragmentation of the H_2O_2 onto $m/e = 33$ could be easily corrected by simultaneously measuring the $m/e = 33$ ion signal, due to HO_2 and H_2O_2, and the H_2O_2 parent ion signal at $m/e = 34$. The fragmentation ratio, $m/e = 33$:$m/e = 34$, of H_2O_2 was then used to correct the $m/e = 33$ ion signal.

In addition, when using O_3 as the ClO precursor, corrections were made for $m/e = 33$ (^{17}OO) and $m/e = 34$ (^{18}OO) to account for the fragmentation of O_3, and production of O_2 in the reaction of Cl with O_3. This correction was <4% of the usual correction for, e.g., $^{13}CH_3OH/^{17}OO$.

To determine the most favorable conditions for the production of HO_2 in the injector, experiments were carried out in which the HO_2 signal was measured as a function of added CH_3OH or HCHO and O_2, for a given Cl atom concentration, or H_2O_2 for a given F atom concentration. For the CH_3OH and HCHO precursors a plateau in the increasing HO_2 signal with added O_2 and CH_3OH or HCHO was taken as a criterion for optimized production. A further check to ensure that no CH_2OH or HCO radicals were entering the main reactor was made by measuring the influence on HO_2 production of Cl_2 added through the

reactor side arm. Reactions 10 and 11 lead to production of Cl

$$CH_2OH + Cl_2 \rightarrow Cl + ClCH_2OH \quad (10)$$

$$HCO + Cl_2 \rightarrow Cl + ClCHO \quad (11)$$

atoms outside of the injector and thus to a rising HO_2 signal with reaction time through reactions 8 + 10 or 9 + 11. In addition, measurement of ion signals for $ClCH_2OH$ ($ClCH_2O^+$ at $m/e = 65$), or ClCHO ($COCl^+$ at $m/e = 63$), were good indicators of nonoptimized source chemistry.

For the H_2O_2 precursor, the possible secondary chemistry arising from H_2O entering the injector was assessed using a detailed numerical simulation.[20] The reaction of F atoms with H_2O to produce OH radicals was a concern as any OH radicals that exit the injector could react with ClO, or its precursors (Cl_2O, OClO, or O_3), in the main reactor to form HO_2, or other unwanted products:

$$H_2O + F \rightarrow OH + HF \quad (12)$$

$$OH + ClO \rightarrow Cl + HO_2 \quad (13)$$

It was found through numerical simulation that the OH production was small ([OH] < 1×10^{10} cm^{-3} for $[F]_0 = 4 \times 10^{11}$ cm^{-3}) if the H_2O_2 purity was >90%. Further simulations showed that, at these low concentrations, reaction of the OH radicals with H_2O_2 or OClO produced immeasurably small perturbation to the first-order decays. To ensure that the majority of the F atoms were consumed, however, required relatively high H_2O_2 concentrations. This also limited the lowest temperature at which the H_2O_2 precursor could be used to 233 K. Below this temperature the required H_2O_2 concentration was above its saturation vapor pressure. As a further test to ensure complete consumption of F atoms, the HO_2 production was monitored as a function of reaction time. An increase in HO_2 concentration with reaction time was observed when $[H_2O_2]_0/[F]_0$ was too low to titrate all the F atoms and OH radicals within the injector. In this case slow HO_2 production occurs outside of the injector due to the reaction of either F atoms or OH with H_2O_2 that had been diluted after leaving the injector and mixed with the bulk carrier gas flow.

Generation and Detection of ClO. ClO radicals, generated by the reaction of Cl atoms with O_3, Cl_2O, or OClO, were added to the reactor via a fixed side arm positioned at the upstream end of the flow tube, and detected as the parent ion at $m/e = 51$.

$$Cl + O_3 \rightarrow ClO + O_2 \quad (2)$$

$$Cl + Cl_2O \rightarrow ClO + Cl_2 \quad (14)$$

$$Cl + OClO \rightarrow ClO + ClO \quad (15)$$

Rapid titration (typical half-lives 0.3−4.0 ms) of Cl to ClO was ensured in each case by the large rate constants of these reactions ($k_{(2)} = 1.2 \times 10^{-11}$, $k_{(14)} = 9.8 \times 10^{-11}$, and $k_{(15)} = 5.8 \times 10^{-11}$ cm^3 s^{-1} at 298 K[21]) combined with sufficient excess concentrations of the molecular precursors.

Despite the low electron energies employed in these experiments (15−25 eV), Cl_2O significantly fragmented onto $m/e = 51$. To measure the coincident parent ion signal due to ClO radicals, the fragmentation pattern of Cl_2O was required. The ratio $m/e = 51$ (ClO^+) : $m/e = 86$ (Cl_2O^+) was therefore measured once for every kinetic run after both discharges were disabled. The size of this correction was generally close to 40%, though frequent measurement of the fragment pattern enabled it to be carried out to an estimated accuracy of ±3%. The same correction process was carried out for OClO, by measuring the ratio $m/e = 51$ (ClO^+) : $m/e = 67$ ($OClO^+$).

Signal Calibration. Although the concentration of HO_2 does not have to be accurately known in kinetic experiments, its measurement helps to confirm that pseudo-first-order conditions are established. The concentration of HO_2 in the main reactor (in the absence of ClO or ClO precursors) was estimated by titration with excess NO. With the injector at the uppermost position (50 cm) NO was added to a side arm inlet near the top of the flow tube. The NO_2 product signal was measured and compared to NO_2 signals from a calibration bulb. The NO_2 mixing ratio in the calibration bulbs (which were also used for the ClO calibrations; see below) were periodically checked using a UV spectrometer and found to be within ±6% of the manometrically determined mixing value. Assuming a stoichiometry of 1 for the conversion of HO_2 to NO_2, $[HO_2]$ could be calculated.

$$HO_2 + NO \rightarrow OH + NO_2 \quad (16)$$

This stoichiometry condition is fulfilled only if the resulting OH does not regenerate any species that can lead to more NO_2 formation, for example, HO_2. By choosing NO concentrations sufficiently high, the OH radical product reacts predominantly with NO instead of CH_3OH, HCHO, or H_2O_2.

$$OH + NO + M \rightarrow HONO + M \quad (17)$$

Absolute ClO concentration measurement, necessary for the kinetic analysis, was achieved by adding NO to a side arm inlet near the top of the flow tube and measuring the resultant NO_2 signal at $m/e = 46$.

$$ClO + NO \rightarrow NO_2 + Cl \quad (18)$$

$k_{(18)} = 1.7 \times 10^{-11}$ cm^3 s^{-1} at 298 K.[21]

Sufficient NO was added to ensure complete removal of ClO. The titration of ClO was performed under conditions of complete conversion of Cl_2O, OClO, or O_3 to ClO by using an excess of Cl atoms. This prevents re-formation of ClO via reaction of Cl atoms formed in reaction 18 with Cl_2O, OClO, or O_3. During the ClO titration experiments, the HO_2 source was disabled (discharge off) and the flow of HO_2 precursor stopped. For both the Cl_2O and OClO precursors, the temperature dependence for the conversion efficiency of ClO to NO_2 was measured. The ratio of ClO $m/e = 51$ (without NO) to NO_2 $m/e = 46$ (with excess NO) remained constant from 294 to 223 K, as shown in Figure 2A for the OClO precursor. This demonstrated that this titration method works at all temperatures of this study. Also, the spectrometer sensitivity to NO_2, at $m/e = 46$, from the calibrated flow of NO_2, and ClO from a range of titration experiments was found to be linear over a wide range of concentrations (see Figure 2B,C). Typical reactor concentrations (cm^{-3}) of radical and precursor species were $[ClO]_0 = (1-30) \times 10^{12}$, $[HO_2]_0 = (3-5) \times 10^{11}$, $[CH_3OH] = (3-5) \times 10^{13}$, $[HCHO] = (3-5) \times 10^{13}$, $[H_2O_2] = (4-8) \times 10^{12}$, $[O_2] = (1-2) \times 10^{14}$, $[Cl_2O]_0 \approx (3-30) \times 10^{12}$, $[OClO]_0 \approx (4-60) \times 10^{12}$, $[O_3]_0 \approx (1-10) \times 10^{13}$.

Kinetic Experiments. All experiments were carried out under pseudo-first-order conditions with the ClO radical in large excess. Variable reaction times were obtained by the software-controlled translation of the sliding injector over a maximum distance of ca. 50 cm. Usually seven data points were measured, at each point ion signals at $m/e = 33$ (HO_2^+ and precursor/product fragments), 51 (ClO^+), and 86 (Cl_2O^+) or 67 ($OClO^+$)

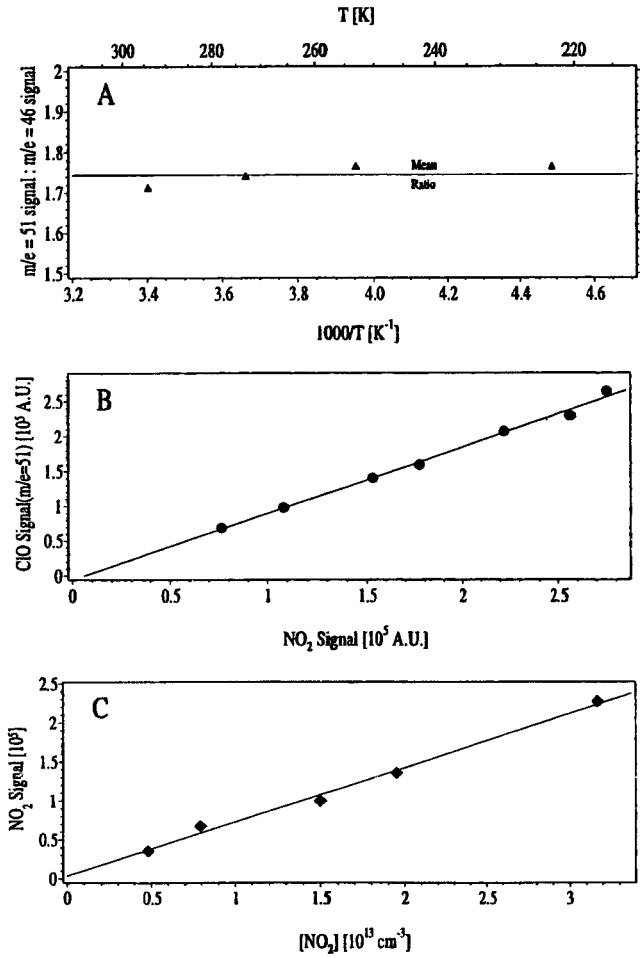

Figure 2. (A) Conversion efficiency of ClO radicals ($m/e = 51$) into NO_2 ($m/e = 46$) using excess NO, between 294 and 223 K. (B) Dependence of NO_2 formed in the NO + ClO reaction on the initial ClO. (C) NO_2 calibration curve for the mass spectrometer.

or 48 (O_3^+) were monitored. For experiments using the H_2O_2 precursor, the $m/e = 34$ ($H_2O_2^+$) and, in some experiments, the $m/e = 52$ ($HOCl^+$) ion signals were also monitored.

As Cl_2O, OClO, or O_3 was only partially converted to ClO, a sufficiently high concentration was usually present in the main flow tube during kinetic runs to scavenge Cl produced by the self-reaction of ClO. Numerical simulation suggested that, at low excess concentrations of Cl_2O, OClO, or O_3, the in situ formation of Cl atoms is sufficient to generate significant HO_2 in the main reactor when using the CH_3OH and HCHO precursors via reactions 8 + 5a or 9 + 6, respectively. This effect is discussed in detail later.

Generally, $[Cl_2O]_0$, the Cl_2O concentration entering the reactor after partial titration with Cl atoms, was kept equal to ca. $[ClO]_0$; i.e., only 50% of the input Cl_2O was consumed. This value represents a compromise between keeping the concentration of Cl_2O sufficiently high to rapidly scavenge Cl atoms and at the same time reducing the size of the Cl_2O ion fragment at $m/e = 51$ (see below). $[O_3]_0$ was generally used in around 3-fold excess of $[ClO]_0$ as its reaction with Cl is the slowest of the three precursors. $[OClO]_0$ was usually $(1-2)[ClO]_0$.

Product Measurements. Two sorts of experiments were carried out to assign ion signals to products of reaction 3. In the first, the injector was translated as in a normal kinetic experiment, and product peaks were monitored at each injector position. This was carried out for the already established HOCl product.

Alternatively, products could be identified by their modulated signals upon turning either one or both discharges off. All three ClO precursors, Cl_2O, OClO, and O_3, were used to eliminate systematic errors resulting from unknown source chemistry.

Materials. The gases and purification methods employed in these experiments were as follows: He (99.999%) was passed through a liquid nitrogen trap and an oxysorb column. O_2 (99.999%), F_2 (0.15% mixture in He), and Cl_2 (2% mixture in He) were obtained from commercial suppliers and used without further purification. CH_3OH (HPLC grade) was thoroughly degassed before use. NO (99.5%) was purified by fractional distillation to remove all traces of NO_2 and higher oxides. After purification the NO froze as a colorless solid at 77 K, and its mass spectrum revealed ≪1% levels of NO_2 impurity. The preparation and purification of NO_2, Cl_2O, O_3, and OClO have already been discussed in a previous publication.[19] The NO_2 was diluted to 1% in 300 Torr of He. The low partial pressure of NO_2 ensured that formation of N_2O_4 was negligible, thus eliminating the need to correct for its dissociation in the flow tube.

The HCHO flow was generated and controlled in situ by flowing He (a regulated flow of ca. 25 sccm) through a gently heated (333−353 K) column of paraformaldehyde. The partial pressure of HCHO was then controlled by passing the HCHO/He mixture through a glass trap, cooled to a constant temperature of usually ca. 153 K, and simultaneously regulating the total pressure. The pressure was monitored using a capacitance manometer upstream of the paraformaldehyde column and actively regulated using a Teflon needle valve downstream of the trap. Cooling the HCHO/He mixture also served to remove the water and any polymerized $(HCHO)_x$. This flow was then further diluted by a second He flow of ca. 200 sccm. The further reduction in HCHO concentration eliminated HCHO condensation and provided a stable and easily controllable HCHO concentration in the injector.

An 85% H_2O_2 solution was further purified to around 95% by vacuum distillation at 273 K before use. The delivery of a controlled flow of H_2O_2 into the injector was achieved by regulating the total pressure in a thermostated (278 K) bubbler of H_2O_2 supplied with a constant He flow. This ensured that the partial pressure of H_2O_2 in the He gas stream remained fairly stable. The pressure upstream of the bubbler was monitored, to prevent contact of the H_2O_2 with metal surfaces, and regulated downstream using a Teflon needle valve. The H_2O_2 was gently pumped overnight between experiments to maintain the high purity.

Results

Kinetics. The total rate constant for the reaction between HO_2 and ClO was measured by monitoring HO_2 concentration profiles under pseudo-first-order conditions, i.e., $[HO_2] = (3-5) \times 10^{11}$ cm^{-3} and $[ClO] = (1-30) \times 10^{12}$ cm^{-3}. The first experiments were carried out at total pressures of 1.1 and 1.7 Torr of He. Subsequently the majority of experiments were performed at total pressures in the range 1.45−1.55 Torr of He. Of the nine possible combinations of HO_2 and ClO source, seven were employed to produce kinetic data. Experiments using O_3 as a ClO precursor are, however, discussed separately.

Assuming pseudo-first-order kinetics, decay rates k_{obsd} are obtained from the slopes of plots of ln(HO_2 signal) versus time as shown in Figure 3A−C. The absence of a systematic variation of the ClO concentration over the entire reaction zone was taken as confirmation of pseudo-first-order kinetics.

First-order decay rates of HO_2 in the absence of ClO but with the ClO precursor present were observed to be on the order of

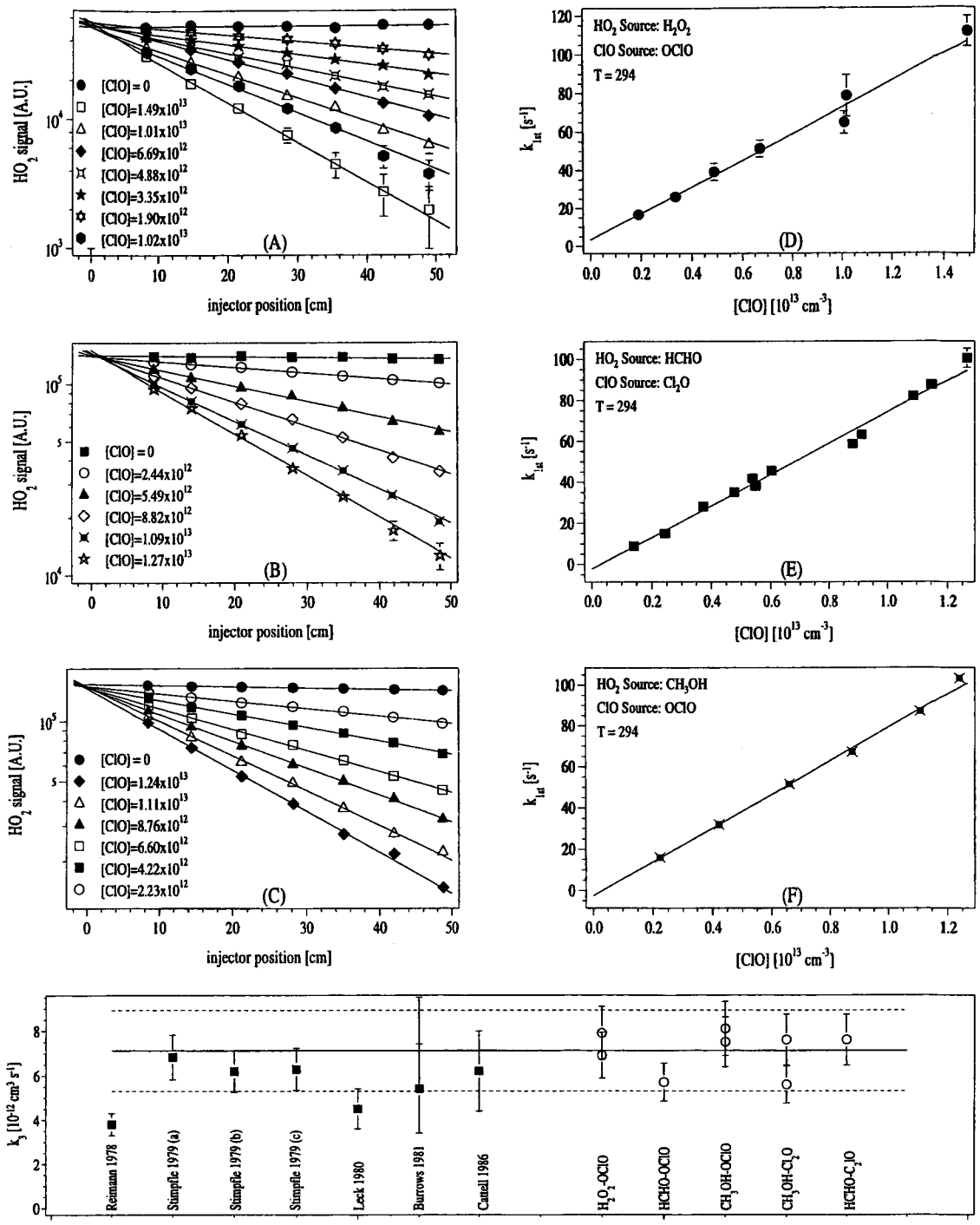

Figure 3. (A−C) Typical first-order data (including estimated measurement precision, ±1000 HO_2 signal counts). (D−F) respective, resulting second-order plots (±2σ in the first-order rates). The rate constants obtained are (6.9 ± 0.5), (7.6 ± 0.1), and (8.1 ± 0.2) × 10^{-12} cm^3 s^{-1} for (D), (E), and (F), respectively. The bottom panel summarizes the present work (open circles) and published data (filled squares) obtained between 294 and 303 K. Error bars are the ±2σ uncertainties in the rate constants. The solid line and dotted lines (2σ errors) represent the present result of (7.1 ± 1.8) × 10^{-12} cm^3 s^{-1}. The data from Stimpfle et al.[11] marked a−c refer to three different flow tube diameters.

2−4 s^{-1} due to a combination of HO_2 self-reaction, reaction with impurities formed in the discharge (e.g., NO), and potentially a small extra component due to wall loss.

Measured HO_2 first-order decay constants k_{obsd} were corrected for diffusion effects[22] to give k_{1st}. Generally the correction for diffusion was around 2%, reaching a maximum of 4% at the lowest temperatures. Assuming no wall loss, the bimolecular rate constant ($k_{(3)}$) is related to k_{1st} by eq i. The rate constant

$$k_{(3)} = k_{1st}/[ClO]_0 \qquad \text{(i)}$$

$k_{(3)}$ was derived from linear plots of k_{1st}, corrected for the measured loss of HO_2 in the absence of ClO, versus $[ClO]_0$ at each temperature, e.g., Figure 3D−F. The rate constants were obtained by least-squares fitting, weighted by the error in the first-order decays.

Experiments at 294 K (OClO and Cl_2O Precursors). Once corrected for precursor fragments falling onto $m/e = 33$, the HO_2 decays at 294 K were observed to be exponential (e.g., Figure 3). The 294 K results for $k_{(3)}$ are listed in Table 1. The quoted errors are 2σ confidence limits from the fitting procedure.

TABLE 1: Rate Constants for the Reaction HO_2 + ClO → Products at 294 ± 1 K

precursor combination	[ClO][a]	no. of decays	k_{2nd}[b] (±2σ)
CH_3OH/Cl_2O	4−24	11	5.6 ± 0.2[c]
CH_3OH/Cl_2O	3−18	13	7.6 ± 0.2
HCHO/OClO	2−20	9	5.7 ± 0.1
$HCHO/Cl_2O$	1.4−13	14	7.6 ± 0.1
CH_3OH/OClO	2.0−12	6	8.1 ± 0.2
CH_3OH/OClO	2.0−12	7	7.5 ± 0.2
H_2O_2/OClO	1.9−15	8	6.9 ± 0.5
H_2O_2/OClO	1.8−11.0	11	7.9 ± 0.4
H_2O_2/O_3	1.8−9.8	8	7.5 ± 0.4
CH_3OH/O_3	3−17	10	8.0 ± 0.4
CH_3OH/O_3	2−20	6	10.0 ± 0.1
	av (excluding O_3 data):		7.1 ± 1.8

[a] Units 10^{12} cm^{-3}. [b] Units 10^{-12} cm^3 s^{-1}. Rate coefficients obtained using the same precursor pairs, but measured at different times during the course of the study, are not averaged, but presented separately.[c] The final result combines data measured at 1.1 and 1.7 Torr of total pressure.

TABLE 2: Rate Constants for the Reaction HO_2 + ClO → Products[a]

T/K	precursor combination	[ClO][b]	no. of decays	k_{2nd}[c] (±2σ)
333	H_2O_2/O_3	2.4−9.8	7	6.7 ± 0.6[d]
333	CH_3OH/O_3	2−15	7	8.6 ± 0.1[d]
269	CH_3OH/Cl_2O	3−12	6	6.8 ± 2.0
269	CH_3OH/Cl_2O	5−20	10	5.0 ± 0.3[e]
269	$HCHO/Cl_2O$	1.5−13	7	5.8 ± 0.1
253	H_2O_2/OClO	1.6−13.2	12	6.6 ± 0.5
247	CH_3OH/Cl_2O	5−22	10	7.0 ± 0.6[e]
243	H_2O_2/OClO	1.6−24.1	9	6.8 ± 0.5
233	$HCHO/Cl_2O$	5−22	7	7.8 ± 0.2
233	H_2O_2/OClO	1.4−27.4	12	7.7 ± 0.8
233	H_2O_2/O_3	1.1−18.6	13	8.4 ± 0.9[d]
233	H_2O_2/O_3	1.0−15.5	13	10.5 ± 1.0[d]
230	CH_3OH/Cl_2O	5−22	10	6.5 ± 0.6[e]
223	CH_3OH/Cl_2O	4−22	15	6.5 ± 0.4
223	HCHO/OClO	5−22	13	7.3 ± 0.2
223	CH_3OH/OClO	5−21	6	5.8 ± 0.3
223	CH_3OH/O_3	1.3−13	5	14.0 ± 0.8[d]
223	CH_3OH/O_3	1−20	9	11.1 ± 0.5[d]
223	CH_3OH/O_3	1−10.4	6	8.7 ± 0.3[d]
215	CH_3OH/Cl_2O	5−23	9	6.6 ± 0.4[f]

[a] Except where noted total pressure was between 1.45 and 1.55 Torr. [b] Units: 10^{12} cm^{-3}. [c] Units: 10^{-12} cm^3 s^{-1}. Rate coefficients obtained using the same precursor pairs, and at the same temperature, but measured at different times during the course of the study are not averaged, but presented separately. [d] O_3 data not included in final analysis of the reaction temperature dependence. [e] The final result combines data measured at 1.1 and 1.7 Torr of total pressure. [f] Total pressure 1.3 Torr.

By propagation of the errors involved in calculating the bimolecular rate constant,[22] the precision of our results may be estimated. The major contributors to an overall precision of around ±15% at all temperatures are the $[ClO]_0$ measurement (±12% was the greatest observed discrepancy between two consecutive titrations) and the fit to the HO_2 decay (±5%). The consistently high-quality data obtained at 294 K using Cl_2O and OClO precursors are exemplified in Figure 3. The room-temperature rate constant from this work is $(7.1 \pm 1.8) \times 10^{-11}$ cm^3 s^{-1}.

Kinetics at T < 294 K (OClO and Cl_2O Precursor). The first experiments in this study were carried out using the CH_3OH/O_2 + Cl_2O precursor combination. These data, measured at total pressures of 1.1 and 1.7 Torr, are summarized in Table 2. Within this pressure range, there is no discernible pressure dependence in the rate constant at any temperature. The temperature dependence of the rate constant was, however, not in agreement with that previously measured,[11] which prompted a thorough investigation of possible systematic errors.

At and above 253 K, the HO_2 signals obtained at high ClO concentrations were observed to decay exponentially to zero. There was no reduction in the quality of the data obtained at these lower temperatures when compared to 294 K as the HO_2 sources were unaffected by the reduced temperature. It was found that, in the temperature range 253 K ≥ T ≥ 215 K, the HO_2 signal (corrected as described above) did not decay to zero at long reaction times and high ClO concentrations. This nonexponential decay was interpreted as the formation of *inert* species, in the HO_2 injector, which provided an additional *residual* signal at $m/e = 33$. The origin and nature of the inert species that caused these residual signals at low temperatures are discussed later.

The size of the residual signal was determined by titration of the HO_2 using high concentrations of ClO and long reaction times. Once the HO_2 had been fully titrated, further increases in the ClO concentration did not alter the magnitude of the residual, demonstrating that the species responsible was formed predominantly in the HO_2 injector and, very importantly, was not reactive toward ClO. Since the species responsible for these residual signals proved to be inert to ClO, subtraction of this additional residual signal was a legitimate correction to the $m/e = 33$ signal profiles, provided it is made in the injector. Note also that addition of a high concentration of NO (10^{14} cm^{-3}) into the reactor *in the absence of ClO* did not influence the size of the residual signal (see later). Subtracting this residual (in addition to the usual correction) from *all* the $m/e = 33$ signals, regardless of [ClO] and reaction time, resulted in exponential decay profiles within experimental precision (Figure 4). Furthermore, the resulting second-order behavior becomes linear. The change to the initial slope, i.e., at low [ClO], of the original curved second-order plots was small, the correction only significantly modifying the high [ClO] points. For an example of the corrected first- and second-order plots see Figure 5. Note that the uncorrected first-order decay rates in the lower panel of Figure 5 were obtained from the initial slope of the HO_2 signals that were not corrected for the residual, but corrected for precursor fragmentation as previously described.

It was impossible to measure the residual at the shorter reaction times used in these experiments, as the very high ClO concentrations required for titration of the HO_2 at short reaction times could not be generated. Thus, the time dependence of the residual remained undefined in the range from 8 cm (first measurement point) to around 30 cm, approximately halfway along the flow tube. Because of this, the effect of subtracting a time-dependent residual upon the first-order decays was examined. An exponential growth function was used to simulate the formation of a product in the flow tube that could potentially result in a time-dependent residual signal. The first-order growth rates for this residual signal were chosen to be sufficiently fast to reproduce the constant residual signal measured at the longer reaction times. Subtraction of a time-dependent residual in this manner had little effect upon the first-order decay rate obtained by applying the normal correction for a time-independent residual, due, e.g., to an unreactive species emerging from the reactor.

The experiments carried out using Cl_2O and OClO precursors for ClO, and all three HO_2 precursors, provide a consistent set of data in the temperature range 298 K ≥ T ≥ 215 K, (see Figure 6). Because of uncertainties surrounding the use of O_3 as a ClO precursor (see below), the O_3 data were not included

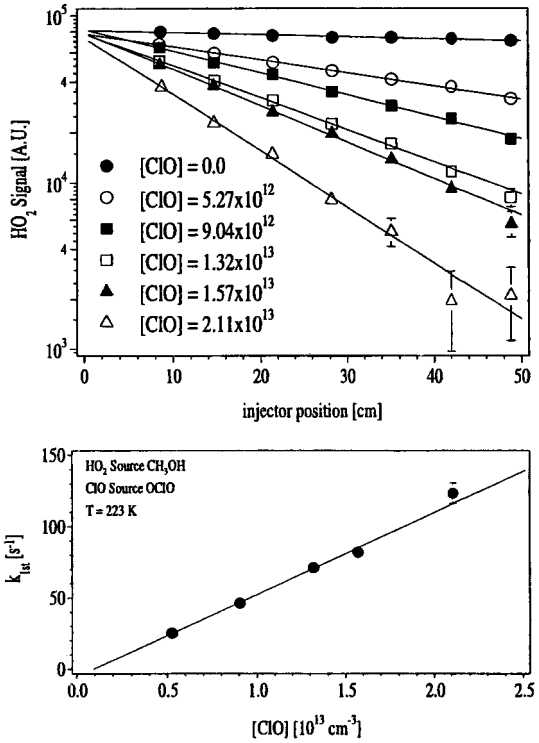

Figure 4. Upper panel: HO_2 decays from experiments carried out at 223 K using CH_3OH and OClO as the HO_2 and ClO sources, respectively. Decays have been corrected for *residual* signals as described in the main text, ClO concentration in units of cm^{-3}. Error bars show an estimated measurement precision of ± 1000 HO_2 signal counts. Lower panel: k_{1st} versus [ClO] from the data in the upper panel, to give a rate constant of $(5.8 \pm 0.3) \times 10^{-12}$ cm^3 s^{-1}. Error bars are the $\pm 2\sigma$ uncertainty in the first-order decays.

in the final analysis. The measured temperature dependence for the reaction between HO_2 and ClO is described by the Arrhenius expression ($\pm 2\sigma$):

$$k_{(3)}(298\ \text{K} < T < 215\ \text{K}) = (7.1 \pm 0.4) \times 10^{-12} \exp(-16 \pm 17/T)\ \text{cm}^3\ \text{s}^{-1}$$

The uncertainty in $k_{(3)}$ at each temperature is expected to be around $\pm 15\%$.[22]

Experiments with O_3 Precursor. The results from all the experiments with O_3 precursor are also summarized in Tables 1 and 2. Data obtained in the lower temperature range (253 K $\geq T \geq$ 223 K) were corrected for the residual signals in the same manner as described above for the Cl_2O and OClO precursor experiments. Again, subtracting these residuals, measured by using excess ClO, results in linear exponential decays and a linear dependence of the decay rate on [ClO].

Although the data obtained using O_3 precursor were of quality equal to that of the data obtained with Cl_2O and OClO precursors, the rate constants measured at all temperatures were systematically larger and had a greater scatter. This is particularly apparent at lower temperatures, for example, 223 K, where the three experiments with the CH_3OH/O_3 precursor combination give rate constants of 8.7×10^{-12}, 11.1×10^{-12}, and 14.0×10^{-12} cm^3 s^{-1}.

The Arrhenius fit to the data obtained with O_3 as ClO precursor (Figure 6) is given below.

$$k_{(3)}(333\ \text{K} < T < 223\ \text{K}) = (6.6 \pm 0.8) \times 10^{-12} \exp(-85 \pm 18/T)\ \text{cm}^3\ \text{s}^{-1}$$

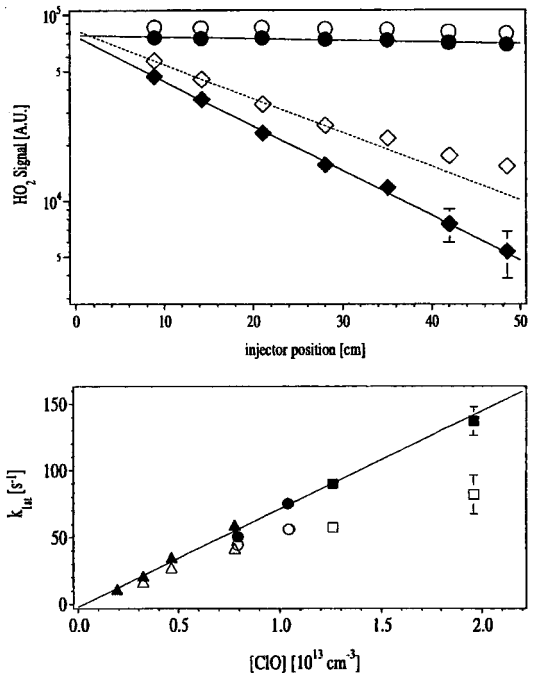

Figure 5. Upper panel: ln(HO_2 signal) at 223 K versus injector position. HCHO was the HO_2 precursor, and OClO the ClO precursor. Open diamonds are the $m/e = 33$ signals measured at [ClO] $= 1.96 \times 10^{13}$ cm^{-3} prior to correction of the nontitratable residual (14 000 counts). Subtraction of a residual of 14 000 counts gives the solid diamonds. The open (uncorrected) and solid (corrected) circles are the HO_2 decays in the absence of ClO. Lower panel: Pseudo-first-order decays constants versus $[ClO]_0$ at 223 K obtained using the HCHO and OClO precursor combination. The open symbols are uncorrected, the filled symbols corrected for the residual at $m/e = 33$. The squares, triangles, and circles are the first-order decays from three separate days of experiments.

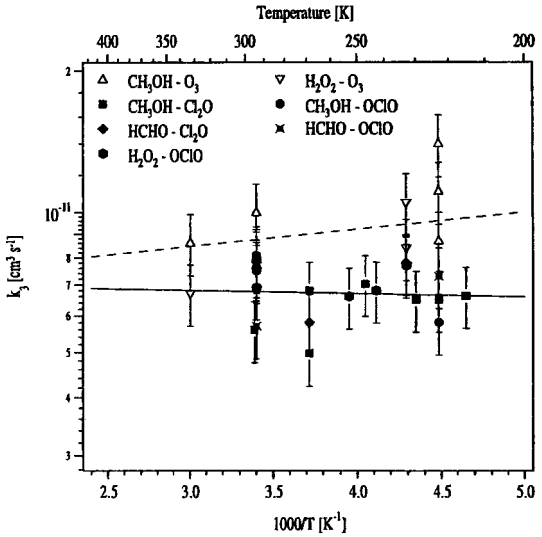

Figure 6. Arrhenius plot of the present data for the reaction of HO_2 with ClO showing results from different HO_2 and ClO radical precursor combinations. Error bars are the $\pm 15\%$ estimated systematic errors.

Product Formation. In light of the strong negative temperature dependence measured by Stimpfle et al.[11] at $T < 298$ K, they proposed that the reaction between HO_2 and ClO occurs by two mechanisms: direct abstraction of H, dominating at high temperature, and formation of a cyclic complex favored at lower temperatures. The formation of HOCl and O_2 via a simple metathesis reaction is also theoretically predicted by Buttar and Hirst.[23] Their ab initio calculations indicate that the reaction

TABLE 3: Exoergic Product Channels for the Reaction between HO_2 and ClO[a]

channel			ΔH_R/(kJ mol^{-1})
3a	$HO_2 + ClO$	$\rightarrow HOCl + O_2$	-189.1 ± 12.6
3b		$\rightarrow HCl + O_3$	-63.6 ± 2.1
3c		$\rightarrow HOClO_2$	-96.2,[b] -118[c]
3d		$\rightarrow HOOOCl$	-75.7[b]
3e		$\rightarrow HOOClO$	-7.9,[b] -31[c]

[a] Values for ΔH_R for reactions 3a and 3b were obtained from ref 21. [b] Reference 17. [c] Reference 18.

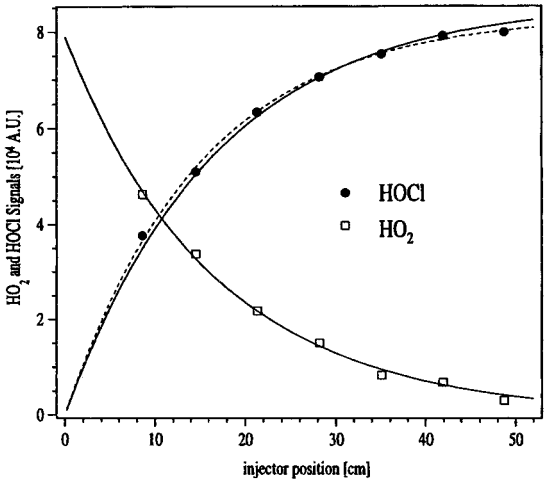

Figure 7. HO_2 decay and the resulting HOCl growth. The dashed line is the fit to the HOCl growth profile using $[HOCl]_t = [HOCl]_\infty(1 - \exp(-kt))$. The solid lines are the fit to the HO_2 decay $[HO_2]_t = [HO_2]_0 \exp(-kt)$ and the growth profile for HOCl employing the same value of k.

proceeds via two mechanisms: direct hydrogen abstraction on a triplet surface with a small, almost zero, activation energy and a multistep reaction on a singlet surface. Although these calculations were not exhaustive, no evidence of a reaction channel forming O_3 and HCl was found. Their calculated singlet surface possesses several local minima that could give rise to long-lived intermediates. However, there are no experimental data to support formation of stable $HClO_3$ isomers by this reaction.

The exoergic or thermoneutral product channels for reaction 3 are listed in Table 3. As already discussed HOCl ($m/e = 52$) has been positively identified in previous studies as the primary product of reaction 3. HOCl growth profiles were measured in many experiments using all precursor combinations. Once corrected for a constant concentration of HOCl coming from the side arm discharge, HOCl profiles displayed first-order production kinetics comparable with the HO_2 removal as shown in Figure 7. A probable source of HOCl in the side arm is reaction of OH radicals (generated in the microwave discharge) with Cl_2 or Cl_2O. The O_3 precursor produced far less HOCl. The magnitude of the correction was generally around 30− 40% of the modulated signal due to $HO_2 + ClO$ reaction, but the correction was occasionally greater due to HOCl impurity in the Cl_2O sample.

The kinetic data from HOCl profiles were obtained by fitting the corrected $m/e = 52$ signal to a first-order rate equation (ii).

$$[HOCl]_t = [HOCl]_\infty(1 - \exp(-kt)) \qquad \text{(ii)}$$

The rate constants obtained by this fitting procedure were highly sensitive to the magnitude and stability of the background signal subtracted from the $m/e = 52$ profiles obtained during the experiments.

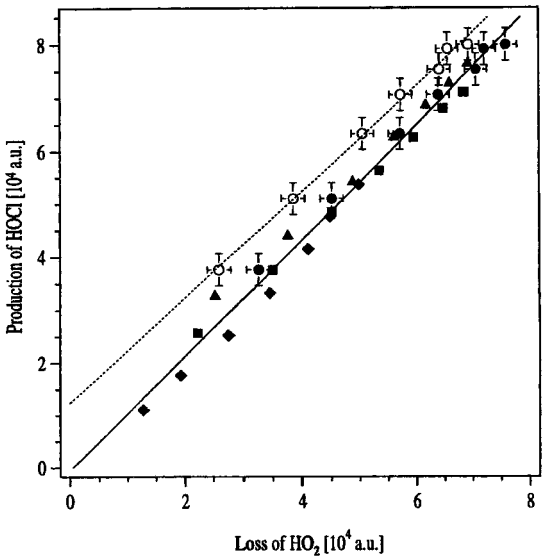

Figure 8. Loss of HO_2 versus production in HOCl. The solid line is a linear fit to the corrected data (filled symbols). Diamonds, $[ClO] = 3.28 \times 10^{12}$ cm^{-3}; squares, $[ClO] = 6.15 \times 10^{12}$ cm^{-3}; triangles, $[ClO] = 7.84 \times 10^{12}$ cm^{-3}; circles, $[ClO] = 1.04 \times 10^{13}$ cm^{-3}. Some of the error bars that represent the estimated measurement precision have been omitted for clarity. The dashed line is a linear fit to the uncorrected data (open circles). The HO_2 precursor was CH_3OH, and the ClO precursor was O_3.

As the first measurement of the HO_2 and HOCl profiles was made at an injector distance of 8 cm, equivalent to reaction times of $(4-7) \times 10^{-3}$ s under typical flow conditions, ∼50% of the HO_2 had already been consumed when using high [ClO]. This characteristic of the experiment was particularly detrimental to the fitting of the HOCl profiles as most of the initial rise in the HOCl signal is not measurable. The result of this is that the injector position corresponding to the true $t = 0$ is also poorly defined. Allowing either the background HOCl signal subtracted from the $m/e = 52$ profiles or a constant offset in the time base to be floated as a second variable in the fitting process sometimes produced dramatically different rates for the formation of HOCl. At worst the formation rates were a factor of 2 larger, although ∼30−40% was more typical. Also, the least-squares fit typically had a 30% uncertainty compared to 3−5% uncertainty for the HO_2 decays. Note that the HOCl growth profiles could in this way always be fitted with the same first-order rate as the corresponding HO_2 decay. This further demonstrates the difficulty in using growth profiles of products to determine kinetic parameters in flow tubes.

Since fitting HOCl growth profiles did not provide unequivocal first-order rate constants, they were not used in isolation to obtain kinetic data. Instead they were used to check that the chemistry resulting in the decay of HO_2 was only dependent upon the ClO concentration and not upon other species or effects. This was achieved by plotting the loss of HO_2 (difference in the HO_2 signal measured in the absence and presence of ClO) versus the gain in HOCl (after background subtraction), thus eliminating the uncertainty in the time base. An example is given in Figure 8, which shows a linear relationship and demonstrates that the loss of HO_2 was directly proportional to the HOCl formation after correction of the HO_2 signals. This was found to be the case at all temperatures. Most importantly, it demonstrated that the subtraction of a residual signal from the HO_2 decays at low temperatures (the data in Figure 8 are from experiments at 223 K) was appropriate.

Formation of O_3 and HCl from the reaction of HO_2 with ClO is of considerable interest both theoretically and with respect

to atmospheric modeling of stratospheric ozone loss. A mechanism for O_3 and HCl formation must involve a complex mechanism as the necessary atom transfers can only be realistically achieved via a cyclic intermediate. O_3 formation attributable to reaction 3 could not be detected at any temperature used in these experiments, and so only an upper limit of 1% could be given for reaction 3b. This upper limit was based on the detection limit of O_3 ($\sim 3 \times 10^9$ cm^{-3}) determined using long integration times to maximize the signal-to-noise ratio. It was impossible to detect HCl with great precision due to high background signals at $m/e = 36$ and $m/e = 38$. A previous study from our laboratory at 700 Torr of total pressure (Ar/O_2) has established branching ratios ($k_{(3b)}/k_{(3)}$) of 2% ± 1% at 240 K rising to 5% ± 2% at 210 K.[16] This apparent discrepancy may be resolved by assuming that the formation of O_3 and HCl from the reaction of HO_2 with ClO is a minor, pressure-dependent, channel. All precursor combinations were used during the search for products other than HOCl. A search was made for possible $HClO_3$ isomers, but no ion signals were detected at $m/e = 84$ or 86 for the parent ions [$HOOOCl^+$], or possible fragment ions not obscured by Cl_2 or ClO precursors at $m/e = 83$ or 85 for [$OOOCl^+$], $m/e = 68$ for [$HOOCl^+$], or $m/e = 49$ for [$HOOO^+$].

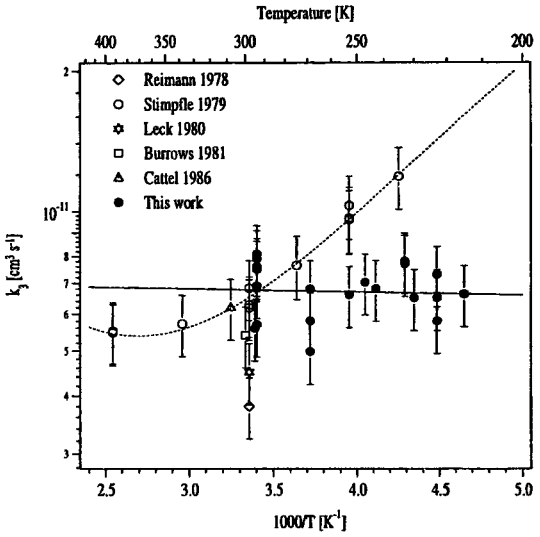

Figure 9. Arrhenius plot of the previously published data. The dotted line is the fit to the data as given by Stimpfle et al.[11] The solid circles are all results for the present study obtained using Cl_2O and OClO as ClO precursors.

Discussion

Comparison of Room-Temperature Data. The room-temperature data can be divided into two groups, those that have determined a "low" rate constant ($k < 5 \times 10^{-12}$ cm^3 s^{-1}) and those that determined a "high" rate constant ($k > 5 \times 10^{-12}$ cm^3 s^{-1}). As can be seen in Figure 3 (bottom panel), our rate coefficient, obtained at 294 K, belongs to the high rate constant group. Reimann and Kaufman[10] used a flow tube and laser-induced fluorescence to detect OH (formed by titration of HO_2 with NO) rather than measurement of HO_2, and obtained a low value for the rate constant of $(3.8 \pm 0.5) \times 10^{-12}$ cm^3 s^{-1} at 298 K. Ozone was the only ClO precursor used. Leck et al.[14] also used a flow tube but measured the HOCl product by mass spectrometry to determine a rate constant of $(4.5 \pm 0.9) \times 10^{-12}$ cm^3 s^{-1}. In that study, the ClO was generated by the reaction of Cl atoms with O_3, and its concentration was determined by monitoring the change in the Cl_2 concentration ($m/e = 70$) and by titration with NO. As the authors point out, and as already discussed, the measurement of product growth rates, to obtain kinetic parameters in flow tubes, is very sensitive to determination of the true reaction time.

The results, at 298 K, from the discharge-flow study of Stimpfle et al.[11] are in good agreement with those from this study and together represent the flow tube contributions to the high rate constant group. We note that a large proportion of the scatter in the results obtained by flow tube studies is probably due to systematic errors made in measuring the ClO concentrations. The use of several different ClO precursors, and careful checks (at several temperatures) of the chemistry that converts ClO to NO_2, should have significantly reduced uncertainties related to [ClO] in the present study. Also in the high rate constant group are the studies of Burrows and Cox[13] and Cattell and Cox,[12] both of which used molecular modulation techniques with optical detection to obtain kinetic parameters at higher pressures.

Use of Ozone as Precursor. When using O_3 as ClO precursor, we were able to obtain exponential decays of HO_2 and a linear relationship between k_{1st} and [ClO], but found that the rate coefficient was enhanced relative to that obtained using Cl_2O and OClO as ClO precursors and also showed more variability. In contrast, Stimpfle et al.[11] did not observe a systematic difference in measured rate constant when using Cl_2O or O_3. The exothermic reaction ($\Delta H_R = -161.5$ kJ mol^{-1})[21] of O_3 with Cl is known to produce highly vibrationally excited ClO radicals that are inefficiently quenched by ~1 Torr of He bath gas.[24] Stimpfle et al.[11] assumed that since the ClO radicals travel down a 105 cm long injector (~7 mm i.d.) they would undergo sufficient wall collisions to quench the excitation. In our experiments the ClO radicals travel through a much shorter and wider tube (18 cm × 14 mm i.d.) into the reactor and undergo approximately a factor of 10 less collisions with the wall.

We hypothesize that the scatter in the rate constants obtained using O_3 as ClO precursor was caused by the slightly varying conditions in each experiment, resulting in different rates of quenching for the vibrationally excited ClO radicals. As both Cl_2O and OClO possess Cl−O bonds with similar vibrational characteristics to the ClO radicals, both should be efficient "resonant" quenchers of any excess vibrational energy in the ClO radicals. Also the reactions of Cl_2O and OClO with Cl produce ClO radicals from far less exothermic reactions ($\Delta H_R = -100.4$ and -11.3 kJ mol^{-1}, respectively).[21] Vibrational excitation in ClO may also be the reason for the systematically higher rate coefficients obtained using O_3 as precursor.

Temperature Dependence. We measured a temperature-independent rate coefficient between 215 and 298 K. In contrast, the only published study of the temperature dependence, from Stimpfle et al.,[11] suggests a marked rise in rate constant with falling temperature (see Figure 9). In the following we compare and contrast important elements of the two experiments to try to understand these differences.

Stimpfle et al.[11] used a discharge-flow reactor with laser magnetic resonance (LMR) detection of the radical species. They report a temperature-dependent wall loss for HO_2, generated in the side arm, on the uncoated outer surface of the injector. This wall loss is negligible above 260 K but increases sharply to 30 s^{-1} at 235 K. This should be compared to total loss rates of between ~50 and 180 s^{-1}. Although this may be coincidental, the onset of this wall loss is in the same temperature range as the sharp increase in their measured rate constants. In the present study, HO_2 is produced in the injector and does not come into

contact with uncoated glass; furthermore, our measured loss rates of HO_2 in the absence of ClO and at all temperatures are less than 4 s^{-1}.

Stimpfle et al.[11] found that on the phosphoric acid coated walls of their flow tubes the loss of ClO was less than 1 s^{-1}. In our study no indication of a systematic ClO wall loss was observed on the uncoated outer surface of the injector. The loss of ClO to the halocarbon wax coated reactor walls was negligible ($\sim$0.8 s^{-1}).

The LMR detection system used by Stimpfle et al.[11] was sensitive only to the radical (paramagnetic) species. By comparison, in our study the raw $m/e = 33$ and 51 signals had to be carefully corrected for various background signals. However, by using three different HO_2 and ClO precursors, by monitoring both HO_2 and the HOCl product, and by monitoring the concentrations of the HO_2 and ClO precursors in the reactor via mass spectrometry, the potential for systematic errors is much reduced. Arguably, Stimpfle et al.[11] also had the "cleanest" HO_2 precursor chemistry, using the reaction of H atoms, generated in a microwave discharge of H_2, with O_2. This precursor chemistry was impossible to use in this study as the O_2 concentration required to convert the H atoms to HO_2 would swamp the $m/e = 33$ signal.

Because of the discrepancy in the temperature dependencies measured by Stimpfle et al.[11] and in the present study, we now discuss in detail potential sources of systematic error in our work, especially those that would result in systematic error at low temperatures. We therefore conducted experiments to examine the origin and nature of the inert species generated in the injector that necessitated corrections to the HO_2 signals at low temperature, the influence of in situ generation of Cl atoms in the flow tube via the ClO self-reaction, and other potentially interfering secondary chemistry.

Influence of the ClO Self-Reaction. Some channels in the ClO self-reaction generate Cl atoms, which in the presence of CH_3OH/O_2 or $HCHO/O_2$ can result in HO_2 formation in the flow tube.

$$ClO + ClO \rightarrow Cl_2 + O_2 \quad (19a)$$

$$\rightarrow OClO + Cl \quad (19b)$$

$$\rightarrow 2Cl + O_2 \quad (19c)$$

$$ClO + ClO + M \rightarrow ClOOCl + M \quad (19d)$$

Numerical simulation of the experiments with $HCHO/O_2$ and CH_3OH/O_2 precursor pairs for HO_2, and all three ClO precursors, suggests that, at higher temperatures (333 K $\geq T \geq$ 273 K), HO_2 generation in the flow tube could be significant. The size of the effect is dependent on the rate of reaction of Cl with O_3, Cl_2O, or OClO relative to reaction with HCHO or CH_3OH. Note that for the H_2O_2 this is not possible as $Cl + H_2O_2$ is too slow.

Indeed, when using the $CH_3OH/O_2 + O_3$ precursor combination at temperatures greater than 273 K, HO_2 regeneration was observed at very high [ClO] ($>1 \times 10^{13}$ cm^{-3}). The degree of HO_2 regeneration was small, equivalent to a few percent of $[HO_2]_0$. These high [ClO] experiments were used only for measuring the true $m/e = 33$ background signal for the CH_3OH precursor. Since the HO_2 regeneration was only seen at high [ClO], the effect at the lower ClO concentrations, used for obtaining kinetic data, was insignificant, the rate of production of Cl being proportional to $[ClO]^2$. Also, note that O_3 is the least effective of the three ClO precursors for scavenging Cl atoms.

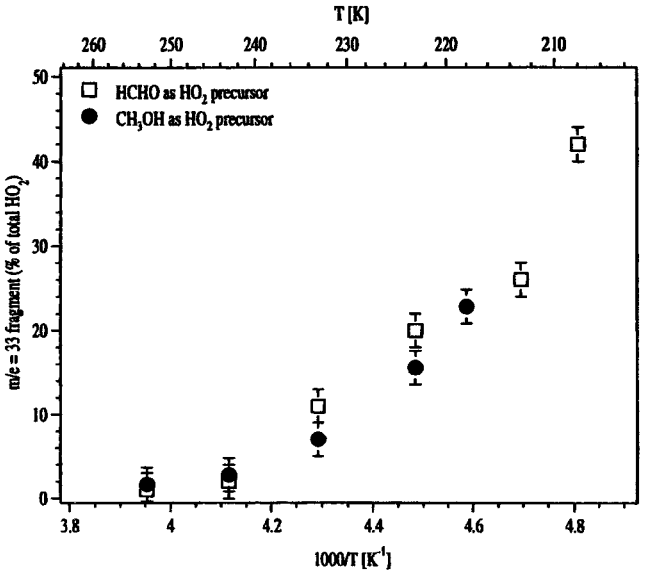

Figure 10. Temperature dependence of the residual signal on $m/e = 33$ for the CH_3OH and HCHO precursors as a percentage of the HO_2 signal.

Two experiments were performed that showed that Cl atom production was insignificant and did not affect the HO_2 decay profiles. First, the $m/e = 33$ (HO_2^+) and $m/e = 52$ ($HOCl^+$) signals were measured with the centerline discharge disabled (HO_2-off) and the sidearm discharge running (ClO-on). No increase in either the $m/e = 33$ (HO_2) or $m/e = 52$ (HOCl) signal with reaction time was observed at any temperature. This was contrary to that expected if Cl atoms formed in the flow tube could react with HCHO or CH_3OH to form HCO or CH_2OH, respectively, both of which would then eventually form HO_2 and then HOCl after reaction with O_2 and ClO. Second, with both discharges running as in a normal experiment, addition of 5×10^{15} cm^{-3} C_3H_8 as a Cl scavenger did not affect the HO_2 decay profile at either 298 or 223 K, although at this concentration of C_3H_8, Cl atoms should be efficiently scavenged.

Possible explanations for the apparent discrepancy between our observations of no significant HO_2 generation and the numerical simulations that predict measurable effects are a reduced rate of Cl atom formation in the ClO self-reactions compared to literature values, and loss of Cl atoms to the uncoated injector, as observed in a previous study with this flow tube.[19]

Origin and Nature of the Residual Signals at $m/e = 33$. The nontitratable residual observed when using the H_2O_2 precursor was 4% of the original HO_2 signal at 253 K, rising to no more than 10% at 233 K. The residual observed with the CH_3OH and HCHO precursors was larger than the H_2O_2 precursor. At 243 K this residual was approximately 2% of the original HO_2 signal, rising to 20% at 223 K. This difference in behavior between the H_2O_2 precursor and both the CH_3OH and HCHO precursors ruled out a common origin. As can be seen in Figure 10, the growth in the residual signal as a function of temperature for both the CH_3OH and HCHO precursors is very similar. It was also observed that the magnitude of the residual signal was dependent upon the reaction time inside the injector. A 50% reduction of the reaction zone length inside the injector, and thus the reaction time, significantly reduced the measured residual for a given temperature.

An observation made when using CH_3OH as a HO_2 precursor was the appearance of signals at $m/e = 45$ and $m/e = 46$. These signals were found to have a temperature dependence identical

to that of the residual signal at $m/e = 33$. Additionally, when CH_3OH was replaced by CD_3OD, these signals were shifted to $m/e = 46$ and $m/e = 48$, respectively, confirming that they originated from ions with one and two hydrogen atoms, respectively. Using CD_3OD as a precursor, the reactivity of the residual species with NO was examined. The signal at $m/e = 48$ was unperturbed by addition of a large concentration of NO ($[NO]_0 > 1.0 \times 10^{14}$ cm^{-3}) to the top of the reactor.

A possible explanation for this residual signal obtained with the CH_3OH precursor is a reaction between CH_2OH and O_2 in which an addition channel to form O_2CH_2OH (reaction 5b) exists at low temperatures. At room temperature, O_2CH_2OH has not been observed as a product of this reaction,[25] although measurements of its temperature dependence indicate the formation of an adduct.[26,27] Nesbitt et al.[26] suggest that O_2CH_2OH can reversibly isomerize to HO_2CH_2O (reaction 20), which,

$$CH_2OH + O_2 \leftarrow M \rightarrow O_2CH_2OH \qquad (5b)$$

$$O_2CH_2OH \leftrightarrow HO_2CH_2O \qquad (20, -20)$$

$$HO_2CH_2O \leftarrow M \rightarrow HO_2 + HCHO \qquad (21, -21)$$

in turn, can dissociate to HCHO and HO_2 (reaction 21). Our observation that the residual at $m/e = 33$ was not reduced by the addition of ClO or NO strongly suggests that it is from a closed shell species, as both NO and ClO are generally reactive toward other radical species (e.g., peroxy radicals).

The reactions of HO_2CH_2O and O_2CH_2OH with HO_2 (reactions 22 and 23) would form the closed-shell species HO_2CH_2OH, which may also fragment onto $m/e = 33$, 45, and 46. Note

$$HO_2 + HO_2CH_2O \rightarrow HO_2CH_2OH + O_2 \qquad (22)$$

$$HO_2 + O_2CH_2OH \rightarrow HO_2CH_2OH + O_2 \qquad (23)$$

that a reaction between the O_2CH_2OH radical and HO_2 has already been studied,[28,29] and its rate coefficient found to have a strong negative temperature dependence with a 230 K rate coefficient of $\sim 10^{-10}$ cm^3 s^{-1}. Combined with the concentration of HO_2 in the injector of $\sim 10^{12}$ cm^{-3}, this reaction will go to completion within the injector. We note that similar observations of formation of a $m/e = 46$ signal and falling HO_2 production efficiency were reported by Larichev et al. when using CH_3OH as a precursor for HO_2.[30]

In experiments carried out with HCHO precursor a signal at $m/e = 46$ was also observed when *elevated* HCHO concentrations were used at low temperatures. If the HCHO concentration was increased by more than 10-fold, then the total $m/e = 33$ signal was observed to increase, but the actual production of HO_2, as determined by titration with ClO, decreased. The reverse reaction (-21) may provide the explanation for the similarity in behavior (Figure 10) of the residual formed with the CH_3OH and HCHO precursors. This reaction produces the same adduct species as the reaction between CH_2OH and O_2 if rapid isomerization (reaction 20) is assumed. The reduction in the HO_2 yield at higher HCHO concentrations observed in this study agrees with this observation, as does the measurement of ion signals at $m/e = 46$ at high [HCHO].

Possible sources for the residual formed using H_2O_2 precursor include the formation of H_2O_2 clusters at the lower temperatures, an interaction between HO_2 and H_2O_2, or perhaps a heterogeneous reaction involving H_2O_2. A search for other ion signals was made, but none were detected, and the origin of the residual remains unknown.

Other Secondary Chemistry. The following reactions are potential sources of unwanted secondary chemistry:

$$ClO + HCHO \rightarrow HOCl + HCO \qquad (24)$$

$$ClO + CH_3OH \rightarrow HOCl + CH_2OH \qquad (25)$$

$$ClO + H_2O_2 \rightarrow HOCl + HO_2 \qquad (26)$$

$$HO_2 + Cl_2O \rightarrow \text{products} \qquad (27)$$

$$HO_2 + OClO \rightarrow \text{products} \qquad (28)$$

$$HO_2 + O_3 \rightarrow OH + 2O_2 \qquad (29)$$

$$HO_2 + Cl_2 \rightarrow \text{products} \qquad (30)$$

Because of the experimental conditions used, none of these reactions were found to perturb the measurement of the kinetic parameters. For reaction 24 ($\Delta H_R = -25 \pm 13$ kJ mol^{-1})[21] an upper limit has already been established for the rate constant of 1×10^{-15} cm^3 s^{-1} at 300 K;[31] thus, the rate of reaction is negligible. Reaction 25 is endothermic ($\Delta H_R = 11 \pm 13$ kJ mol^{-1})[21] and is therefore almost certainly slower than reaction 24. Stimpfle et al.[11] established an upper limit for the rate constant of reaction 26 as 6×10^{-16} cm^3 s^{-1} at 300 K, again making this reaction insignificant. Also no growth in HOCl (or HO_2) with reaction time was observed with the ClO source running and the HO_2 source disabled. For reactions 27−30 no significant perturbation of a HO_2 decay (ClO source disabled) was observed in the presence of Cl_2O, OClO, O_3, or Cl_2.

Conclusions

The kinetic behavior of the reaction between HO_2 and ClO has been investigated in the temperature range 333−203 K at total pressures between 1.1 and 1.7 Torr. The data obtained between 298 and 215 K define a temperature dependence for this reaction that is significantly different from that previously obtained. To a first approximation, the significantly lower rate constant for reaction 3a at low temperatures implies that reactions of both ClO and HO_2 with NO_2 to form the longer lived $ClONO_2$ and HO_2NO_2 may reduce the flux through reactions 1−4 and thus result in reduced O_3 loss rates. Also when the polar stratosphere becomes denitrified during the springtime, a lower value of $k_{(3a)}$ will also result in an increase in the ratios HO_2/OH and ClO/Cl for a given J_{HOCl}, these ratios being strongly influenced by the coupling of reactions 3a and 4. The influence of reduced rate constants at stratospheric temperatures should be an interesting aspect for investigation in modeling studies of stratospheric O_3 chemistry. In contrast to experiments at high pressure, no evidence for a $HCl + O_3$ forming channel (upper limit of 1%) was obtained at any temperature or pressure in this study. Further studies of the kinetics and product branching at low temperatures and appropriate pressures are needed to constrain these important parameters for atmospheric modeling.

Note Added in Proof:

During the final reviewing stage of this manuscript, a further publication on the reaction between HO_2 and ClO appeared in the Journal of Physical Chemistry (Nickolaisen, S. L.; Roehl, C. M.; Blakeley, L. K.; Friedl, R. R.; Francisco, J. S.; Liu, R.; Sander, S. P. *J. Phys. Chem.* **2000**, *104*, 308). The rate coefficient between 203 and 364 K was measured as 2.84×10^{-12} exp{(312 ± 60)/T} cm^3 s^{-1} which gives a room temperature result of $\approx 8 \times 10^{-12}$, in good agreement with

the present data. However, the stronger temperature dependence results in low temperature rate coefficients that are significantly higher than the present determination.

Acknowledgment. We thank the European Union for financial support within the Environment Program (EV5V-CT93-0338, CABRIS), and Dr. I Mozorov for some experimental assistance in an early phase of this research.

References and Notes

(1) *Scientific assessment of Ozone depletion: 1994*; World Meteorological Organization, 1995.
(2) Herman, J. R.; Larko, D. *J. Geophys. Res.* **1994**, *99*, 3483.
(3) Farman, J. C.; Gardiner, B. G.; Shanklin, J. O. *Nature* **1985**, *315*, 207.
(4) Solomon, S.; Garcia, R. R.; Rowland, F. S.; Wuebbles, D. J. *Nature* **1986**, *321*, 755.
(5) Crutzen, P. J.; Arnold, F. *Nature* **1986**, *324*, 651.
(6) Wennberg, P. O.; Cohen, R. C.; Stimpfle, R. M.; Koplow, J. P.; Anderson, J. G.; Salawitch, R. J.; Fahey, D. W.; Woodbridge, E. L.; Keim, E. R.; Gao, R. S.; Webster, C. R.; May, R. D.; Toohey, D. W.; Avallone, L. M.; Proffitt, M. H.; Loewenstein, M.; Podolske, J. R.; Chan, K. R.; Wofsy, S. C. *Science* **1994**, *266*, 398.
(7) Toon, O. B.; Hamill, P.; Turco, R. P.; Pinto, J. *Geophys. Res. Lett.* **1986**, *13*, 1284.
(8) Rodriguez, J. M.; Ko, M. K. W.; Sze, N. D.; Heisey, C. W.; Yue, G. K.; McCormick, M. P. *Geophys. Res. Lett.* **1994**, *21*, 209.
(9) Chance, K.; Traub, W. A.; Johnson, D. G.; Jucks, K. W.; Ciarpallini, P.; Stachnik, R. A.; Salawitch, R. J.; Michelsen, H. A. *J. Geophys. Res.* **1996**, *101*, 9031.
(10) Reimann, B.; Kaufman, F. *J. Chem. Phys.* **1978**, *69*, 2925.
(11) Stimpfle, R. M.; Perry, R. A.; Howard, C. J. *J. Chem. Phys.* **1979**, *71*, 5183.
(12) Cattell, F. C.; Cox, R. A. *J. Chem. Soc., Faraday Trans. 2* **1986**, *82*, 1413.
(13) Burrows, J. P.; Cox, R. A. C. *J. Chem. Soc., Faraday Trans. 1* **1981**, *82*, 1413.
(14) Leck, T. J.; Cook., J. L.; Birks, J. W. *J. Chem. Phys.* **1980**, *72*, 2364.
(15) Leu, M. T. *Geophys. Res. Lett.* **1980**, *7*, 173.
(16) Finkbeiner, M.; Crowley, J. N.; Horie, O.; Müller, R.; Moortgat, G. K.; Crutzen, P. J. *J. Phys. Chem.* **1995**, *99*, 16264.
(17) Francisco, J. S.; Sander, S. P. *J. Phys. Chem.* **1996**, *100*, 573.
(18) Grela, M. A.; Colussi, A. J. *J. Phys. Chem.* **1996**, *100*, 10150.
(19) Helleis, F.; Crowley, J. N.; Moortgat, G. K. *J. Phys. Chem.* **1993**, *97*, 11464.
(20) Curtis, A. R.; Sweetenham, W. P. Report R-12805; Atomic Energy Research Establishment, Oxfordshire, England, 1987.
(21) DeMore, W. B.; Sander, S. P.; Golden, D. M.; Hampson, R. F.; Kurylo, M. J.; Howard, C. J.; Ravishankara, A. R.; Kolb, C. E.; Molina, M. J. *Chemical Kinetics and Photochemical Data for Use in Stratospheric Modelling*; No. 11; Jet Propulsion Laboratory, Pasadena, CA, 1997.
(22) Howard, C. J. *J. Phys. Chem.* **1979**, *83*, 3.
(23) Buttar, D.; Hirst, D. M. *J. Chem. Soc., Faraday Trans.* **1994**, *90*, 1811.
(24) Matsumi, Y.; Nomura, S.; Kawasaki, M.; Imamura, T. *J. Phys. Chem.* **1996**, *100*, 176.
(25) Lightfoot, P. D.; Cox, R. A.; Crowley, J. N.; Destriau, M.; Hayman, G. D.; Jenkin, M. E.; Moortgat, G. K.; Zabel, F. *Atmos. Environ.* **1993**, *264*, 1805.
(26) Nesbitt, F. L.; Payne, W. A.; Stief, L. J. *J. Phys. Chem.* **1988**, *92*, 4030.
(27) Grotheer, H.; Riekert, G.; Walter, D.; Just, T. *J. Phys. Chem.* **1988**, *92*, 4028.
(28) Veyret, B.; Lesclaux, R.; Rayez, M.-T.; Rayez, J.-C.; Cox, R. A.; Moortgat, G. K. *J. Phys. Chem.* **1989**, *93*, 2368.
(29) Burrows, J. P.; Moortgat, G. K.; Cox, R. A.; Jenkin, M. E.; Hayman, G. D.; Veyret, B. *J. Phys. Chem.* **1989**, *93*, 2375.
(30) Larichev, M.; Maguin, F.; Le Bras, G.; Poulet, G. *J. Phys. Chem.* **1995**, *99*, 15911.
(31) Poulet, G.; Le Bras, G.; Combourieu, J. *Geophys. Res. Lett.* **1980**, *7*, 413.